

# Kevlar Fiber–Epoxy Adhesion and Its Effect on Composite Mechanical and Fracture Properties by Plasma and Chemical Treatment

S. R. WU, G. S. SHEU, and S. S. SHYU\*

Department of Chemical Engineering, National Central University, Chung-Li, Taiwan 320, Republic of China

## SYNOPSIS

Kevlar 49 fibers were surface-modified by  $\text{NH}_3^-$ ,  $\text{O}_2^-$ , and  $\text{H}_2\text{O}$ -plasma etching and chlorosulfonation and subsequent reaction with some reagents (glycine, deionized water, ethylenediamine, and 1-butanol) to improve the adhesion to epoxy resin. After these treatments, the changes in fiber topography, chemical compositions of the fiber surfaces, and the surface functional groups introduced to the surface of fibers were identified by SEM, XPS, and static SIMS. Interlaminar shear strength (ILSS) and T-peel strength between the fiber and epoxy resin, as measured by the short-beam test and T-peel test, were remarkably improved by gas plasma and chlorosulfonation (0.1% and 0.25%  $\text{ClSO}_3\text{H}$  at 30 s). However, from the results of similar  $G_{\text{IC}}$  values of the treated and untreated fiber composites, it is clear that the fiber/matrix interfacial bond strength is only a minor contributor to  $G_{\text{IC}}$ . SEM was also used to study the surface topography of the fracture surfaces of composites in T-peel test. It could be seen from SEM observations that the improvement of fiber/matrix interfacial bond strength often accompanied a change in fracture mode from the interface of fiber/epoxy resins to the fiber fibrillation and the resins. © 1996 John Wiley & Sons, Inc.

## INTRODUCTION

The use of plasma and chemical treatment to increase the interfacial bonding of the fiber to the matrix has been known for a considerable time.<sup>1–23</sup> Kevlar aramid [PPTA; poly(*p*-phenylene terephthalamide)] fiber is widely used in the manufacture of advanced composites. This has been due to major advances in composite mechanical properties that have resulted from the use of the stiffness, high fracture strain, and low-density reinforcing fibers. However, the adhesion between Kevlar fibers and most matrices is poor, due to the high crystallinity leading a chemically inactive surface and the relatively smooth surface of the fiber. Fiber-surface modification results in improved wettability, surface

energy, surface roughness, and polar groups on the surface. All these would improve the adhesion between the fiber and matrix.

This study examines the effects of plasma and chemical treatment on the mechanical behavior of Kevlar 49 fiber/epoxy laminates. Scanning electron microscopy (SEM) was used to characterize the changes in fiber topography and the fracture surfaces of fibers. The surface compositions and chemical structures of modified fibers were analyzed by X-ray photoelectron spectroscopy (XPS) and static secondary ion mass spectrometry (SSIMS). The double cantilever beam (DCB) method was used to measure toughness,  $G_{\text{IC}}$ . The short-beam method was used to measure the interlaminar shear strength (ILSS) of laminates. The T-peel test was used to measure the T-peel strength of laminates. After these tests, we can further realize the mechanical and fracture properties of Kevlar 49 fiber composites.

\* To whom all correspondence should be addressed.

## EXPERIMENTAL

### Materials

All the aramid fabrics used in this study were woven from Kevlar 49 fibers [poly(*p*-phenylene terephthalamide)] (PPTA; E. I. du Pont de Nemours) in the form of 1140 denier, style 281. The fabrics were cleaned successively with 1,2-dichloroethane, methanol, and deionized water to remove surface contaminants prior to their use, followed by drying at 100°C in a vacuum oven for 12 h before plasma and chemical treatment. The epoxy resin was a commercial diglycidyl-type resin (Epon 828, Shell) and the curing agent was 4,4'-diaminodiphenylmethane (DDM, Merck). Anhydrous ammonia (99.99%), oxygen gas (99.99%), and deionized water were used for plasma treatment. All the other reagents used for chemical treatment were purchased from Merck.

### Plasma Treatments

Following the cleaning procedure, the aramid fabrics were surface-modified by plasma etching carried out in a SAMCO Model BP-1 bell jar plasma reactor. The gases used for the plasma treatments were ammonia, oxygen, and water vapor. After evacuating to a pressure lower than 8 mTorr, the reactor was purged with each gas for three times and then the chamber pressure was maintained at 0.2 Torr throughout the plasma treatment processes. Pieces of aramid fabric were treated at 30 W of rf (radio frequency, 13.56 Mhz) plasma power in each plasma environment for 15 s to 10 min treatment time. After plasma treatment, the samples were left there for 15 min post-treatment to allow for the decay of residual surface radicals.

### Chemical Treatment

The dried fabric pieces were immersed in a solution of chlorosulfonic acid in dichloromethane with stirring at -10°C and the subsequent reaction of —SO<sub>2</sub>Cl groups were converted to other derivatives by immersion in a solution of the appropriate reagents (e.g., deionized water, glycine, ethylenediamine, and 1-butanol) with stirring at 25°C. The acid concentration and reaction time were varied. Then, the treated fabrics were washed and dried.

### Scanning Electron Microscopy (SEM)

Treated fibers, untreated (control) fibers, and the fracture surfaces of composites were mounted and

gold-coated for subsequent examination in a Hitachi S-2300 scanning electron microscope. Both the surface topography of fibers and the fracture surfaces of composites were investigated to assess and compare the fiber/matrix adhesion and fracture mode for each composite.

### X-ray Photoelectron Spectroscopy (XPS)

XPS data for the treated and untreated specimens were obtained on a Perkin-Elmer PHI 590 SAM/ESCA instrument, equipped with a Digital PDP 11/04 computer using a MgK $\alpha$  ( $h\nu = 1253.6$  eV) X-ray source (a voltage of 12 keV, a wattage of 250 W, and a pressure lower than  $5 \times 10^{-8}$  Pa). Survey scans (0–1000 eV binding energy) to determine the elemental composition of the fibers were run at an analyzer pass energy of 100 eV. High-resolution spectra were obtained at a pass energy of 15 eV. The atomic sensitivity factor (ASF) of the elements was considered in calculating the atomic fraction ratios.

### Static Secondary Ion Mass Spectroscopy (SSIMS)

The static SIMS experiments were performed using a Cameca IMS-4f ion microscope equipped with a Cs<sup>+</sup> ion source and a magnetic sector mass analyzer. The primary ion source was 10 keV Cs<sup>+</sup> operated at a current of 10 pA and at a pressure lower than  $1.5 \times 10^{-9}$  Pa. A defocused beam was rastered over an area of  $50 \times 50$   $\mu\text{m}$ . An electron flood gun set at 4.5 keV was used to minimize sample charging.

### Kevlar/Epoxy Composite Fabrication

Kevlar/epoxy composites were fabricated from untreated, plasma-treated, and chemical-treated fabrics and the diglycidyl-type resin (Epon 828, Shell) and 4,4'-diaminodiphenylmethane (DDM, Merck). The fabrics were impregnated by passing samples through a solution containing the Epon 828, DDM, and acetone mixed in a 4 : 1 : 4.8 weight ratio. The resulting samples were dried at 25°C for 30 min and then at 70°C for 20 min. The impregnated fabric composites (8 piles for the double cantilever beam method, 16 piles for the short-beam method, and 2 piles for the T-peel test) were then cured under ambient conditions for 2 h at 80°C followed by 2 h at 150°C (heating rate, 3°C/min) at a pressure of 150 psi. The mold was cooled to room temperature before the pressure was released. The resin weight fraction in the laminates was approximately 32%. The  $T_g$  of the laminate was about 152°C, which was measured using a 910 differential scan-

ning calorimeter module (DuPont Instruments) at a heating rate of 20°C/min in a nitrogen atmosphere (flow rate = 20 mL/min).

### Interlaminar Fracture Energy

The mode I fracture toughnesses,  $G_{IC}$ , of the laminates is given by the double cantilever beam (DCB) method:

$$G_{IC} = \frac{3PV}{2aB} = \frac{P^2}{2B} \frac{dC}{da} \quad (1)$$

where  $P$  is the applied force in Newtons;  $V$ ; the loadline displacement in mm;  $a$ , the crack length in mm;  $B$ , the specimen width in mm; and  $C$ , the specimen compliance ( $V/P$ ). Beam specimens (8 plies) of dimensions 90 × 11 × 1 mm containing a starter crack implanted between the fourth and fifth layers prior to autoclaving were cut from composite panels. The starter crack consisted of a 15 × 11 mm strip of aluminum foil which had been single-folded and was embedded in one edge of the laminate. Specimens were tested at 25°C on an Instron tester at a crosshead speed of 2 mm/min. Each reported  $G_{IC}$  value is the average of more than 10 successful measurements.

### Interlaminar Shear Strength (ILSS)

The interlaminar shear strength of laminates was determined using the short-beam method by ASTM-D-2344-76. Specimen (16 plies) dimensions were nominally 16 × 11 × 2 mm, with a span to thickness ratio of 5. The condition the test specimen and the test in an enclosed space was maintained at 23°C and 50% relative humidity. Test the specimen at a rate of crosshead movement 0.5 mm/min.

The interlaminar shear strength,  $\tau$ , for the short-beam test is calculated by the expression

$$\tau = \frac{3P}{4Bh} \quad (2)$$

where  $P$  is the maximum load in Newtons;  $B$ , the width of specimen in m; and  $h$ , the thickness of specimen in m. Each reported ILSS value is the average of more than 10 successful measurements.

### T-peel Strength

The T-peel strength of laminates was determined using the T-peel test by ASTM-D-1876-72. Speci-

men (2 plies) dimensions were 90 × 11 × 0.25 mm, with a starter crack implanted between two layers. The condition for the T-peel test is the same as for the short-beam method. The T-peel test was performed by using an Instron, pulling the surfaces apart at a rate of crosshead movement 25 mm/min. The T-peel strength in gw/cm,  $W$ , is calculated from  $W = F/B$ , where  $F$  is the force applied to the joint and  $B$  is the width of the strip. The T-peel strength was the average of more than 10 measurements.

## RESULTS AND DISCUSSION

### Fiber Surface Topography

#### Plasma Treatment

The SEM photomicrographs of untreated and plasma-treated fiber surfaces are shown in Figure 1. The control fiber surface is quite smooth, as seen in Figure 1(a). No significant change in the surface texture can be detected after NH<sub>3</sub>-, O<sub>2</sub>-, and H<sub>2</sub>O-plasma treating at 30 W for 10 min, as seen in Figure 1(b)–(d), respectively. This result is the same as the results obtained by Allred et al.<sup>23</sup> in their NH<sub>3</sub>-plasma studies and Küpper and Schwartz<sup>3</sup> in their Ar-, N<sub>2</sub>-, and CO-plasma studies of aramid (Kevlar 49) fibers, which did not exhibit any change in surface topography after plasma treatment. In our laboratory, Kevlar 149 fibers had been surface-treated with plasma to modify their surface structures.<sup>8–11</sup> All the three plasma treatments roughened the fiber surfaces and the etching abilities among different gases is O<sub>2</sub> > H<sub>2</sub>O > NH<sub>3</sub>. This result is different from the result by using Kevlar 49 fibers, so the etching effects is only a minor contributor to the interfacial bonding of Kevlar 49 fiber to the epoxy in plasma treatment.

#### Chemical Treatment

After the treatment with 0.25% chlorosulfonic acid for 15 s, no change in the surface texture was detected [Fig. 2(a)]. But at higher concentrations of chlorosulfonic acid and longer reaction times, the fiber surfaces were etched more vigorously, as seen in Figure 2(b)–(d). After the treatment with 0.25% chlorosulfonic acid for 5 min, the fibers revealed many fragments on the surface, as seen in Figure 2(b). Fibers treated with 1% chlorosulfonic acid for 2.5 and 5 min showed many shallow and discontinuous grooves along the axial direction of the fiber [Fig. 2(c) and (d)]. The significant change in the topography of the fiber surfaces was due to the in-

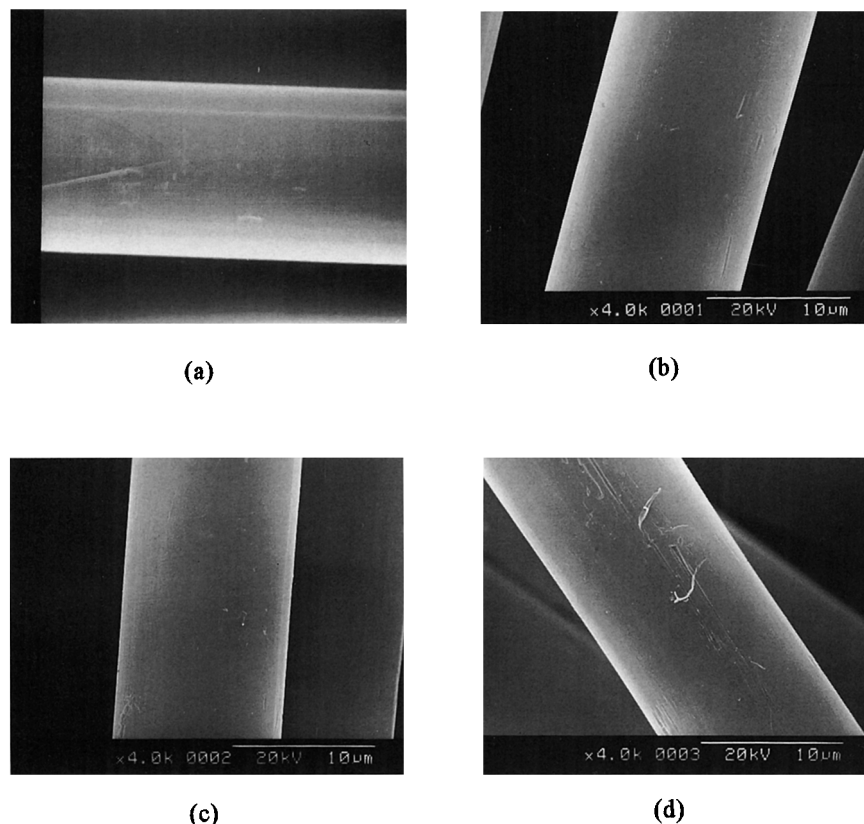


**Figure 1** SEM photographs of Kevlar 49 fiber surfaces treated with different plasma treatments: (a) control; (b) treated by  $\text{NH}_3$ -plasma at 30 W for 10 min; (c) treated by  $\text{O}_2$ -plasma at 30 W for 10 min; (d) treated by  $\text{H}_2\text{O}$ -plasma at 30 W for 10 min.

complete etching by the higher concentration of chlorosulfonic acid. The subsequent treatment of chlorosulfonated fibers (0.25% chlorosulfonic acid for 15 s) with glycine, water, ethylenediamine, and 1-butanol did not detect further change in the fiber-surface topography.

## XPS Analysis

### Plasma Treatment

Kevlar 49 fiber surfaces modified by  $\text{NH}_3$ -,  $\text{O}_2$ -, and  $\text{H}_2\text{O}$ -plasma treatment were analyzed by XPS. Table I summarizes the atomic percentages of carbon, oxygen, and nitrogen and the atom ratios of N/C and O/C for the control and modified fiber surfaces. The chemical composition of Kevlar 49 fibers examined by a Perkin-Elmer Model 2400 elemental analyzer is also listed in Table I. For the theoretical composition of Kevlar 49 fibers, according to the struc-

ture formula (PPTA), there are two oxygen atoms, two nitrogen atoms, and 14 carbon atoms per repeating unit of Kevlar. It can be seen from Table I that the element analysis result for the control fibers is quite in agreement with the theoretical calculation; however, the surface composition of the control fibers is significantly different from the bulk. For the control fiber, the oxygen on the surface is about 2.5 times that in the bulk. The difference may be due to the possible surface oxidation<sup>19,24</sup> and/or surface finishes used during fiber fabrication.

Table I also shows that the surface contents of nitrogen increase from 21.6 to 27.3% after 3 min  $\text{NH}_3$ -plasma treatments at 30 W. This indicates that the nitrogen atoms were incorporated into the fiber surfaces during  $\text{NH}_3$ -plasma discharge. With 30 W  $\text{O}_2$ -plasma treatment for 3 min, the surface oxygen content increases. This can be explained by surface oxidation during the  $\text{O}_2$ -plasma exposure. With 30 W  $\text{H}_2\text{O}$ -plasma treatment for 3 min, the surface

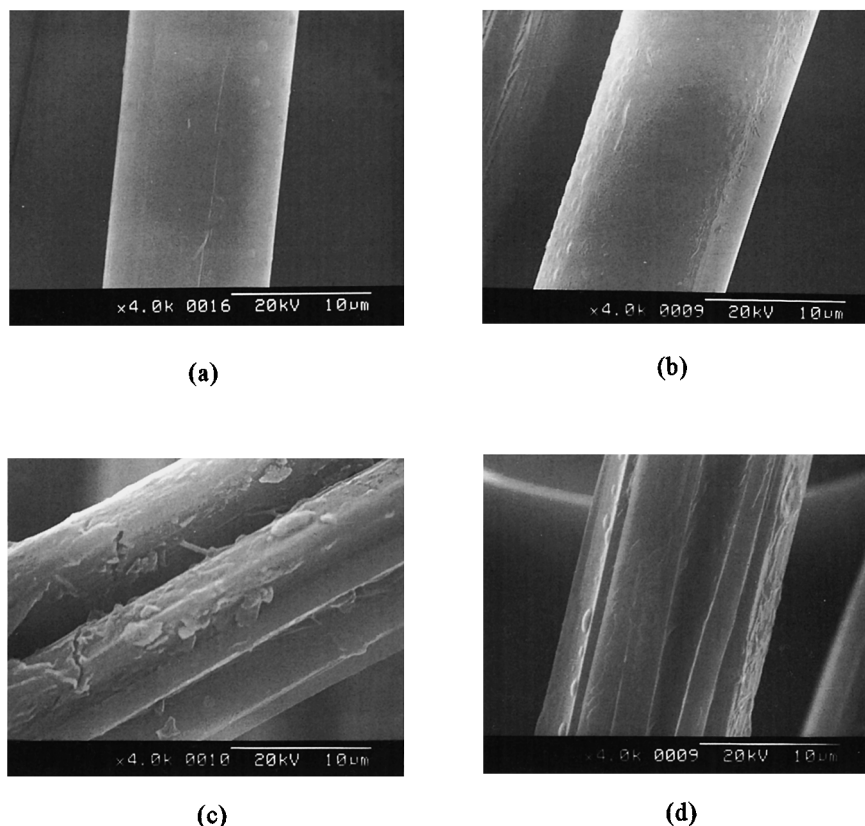


**Figure 2** SEM photographs of Kevlar 49 fiber surfaces treated with  $\text{ClSO}_3\text{H}$ : (a) 0.25%  $\text{ClSO}_3\text{H}$  for 15 s; (b) 0.25%  $\text{ClSO}_3\text{H}$  for 5 min; (c) 1%  $\text{ClSO}_3\text{H}$  for 2.5 min; (d) 1%  $\text{ClSO}_3\text{H}$  for 5 min.

contents of each element were changed. It is evident that the high concentration of atomic oxygen generated in  $\text{H}_2\text{O}$ -plasma was incorporated into fiber surface during plasma discharge.<sup>25</sup>

### Chemical Treatment

The results of chemical treatment are shown in Table II. After chlorosulfonation, the surface contents

**Table I** ESCA Analysis Results of Surface Composition for Plasma-treated Kevlar 49 Fibers

Surface Treatment Conditions	Atomic Percent			Atomic Ratio	
	C	O	N	N/C	O/C
Theoretical	77.8	11.1	11.1	0.143	0.143
EA <sup>a</sup>	74.0	14.4	10.7	0.143	0.192
Control <sup>b</sup>	42.9	35.5	21.6	0.503	0.828
$\text{NH}_3$ -plasma 30 W 3 min	39.2	33.5	27.3	0.696	0.855
$\text{O}_2$ -plasma 30 W 3 min	38.5	42.3	19.2	0.499	1.099
$\text{H}_2\text{O}$ -plasma 30 W 3 min	39.1	37.7	23.2	0.593	0.964

<sup>a</sup> EA: elemental analysis results of the control sample.

<sup>b</sup> Control: 1,2-dichloroethane washed → methanol washed → deionized water washed → dried.

**Table II** ESCA Analysis Results of Surface Composition for Kevlar 49 Fibers

Type of Surface Treatment	Atomic Percent				Atomic Ratio	
	C	O	N	S	N/C	O/C
Theoretical	77.8	11.1	11.1	—	0.143	0.143
Control	42.9	35.5	21.6	—	0.503	0.828
CS	30.7	36.3	12.2	10.0	0.397	1.182
CS + W	36.9	36.6	17.6	14.9	0.570	1.184
CS + G	33.2	44.2	17.9	4.7	0.539	1.331
CS + E	40.6	27.2	25.0	7.2	0.616	0.670
CS + B	51.4	26.0	14.8	7.8	0.288	0.506

CS: chlorosulfonation (0.25% chlorosulfonic acid in dichloromethane for 0.25 min); W: 100% deionized water (hydrolysis) for 15 min; G: 1.0% glycine (in 1,4-dioxane) for 15 min; E: 15% ethylenediamine (in 1,2-dichloroethane) for 15 min; B: 15% 1-butanol (in 1,4-dioxane) for 15 min.

of each element are markedly changed. Another element, sulfur, appeared and the  $-\text{SO}_2\text{Cl}$  groups were formed. The subsequent reaction with glycine, deionized water, ethylenediamine, and 1-butanol also changed the surface composition of the fiber. This procedure may introduce new functional groups on the fiber surface.

## Static SIMS Analysis

### Plasma Treatment

Figure 3(a) reveals the negative SSIMS spectrum of the control fiber surfaces. Although a 1–280 amu mass scan was performed during the spectrum acquisition, the spectrum is dominated by peaks which appear in the mass range less than 100 amu. The negative ion spectra exhibit significant intensities for  $\text{O}^-$  (16),  $\text{OH}^-$  (17),  $\text{CN}^-$  (26),  $\text{O}_2^-$  (32), and  $\text{CON}^-$  (43). The relatively high intensity of oxygen-containing fragments ( $\text{O}^-$ ,  $\text{OH}^-$ , and  $\text{O}_2^-$ ) in the spectrum are observed. This means there is an oxidized layer at the control fiber surface. The high intensity of the peak at 26 amu due to  $\text{CN}^-$  originating from amine group of the PPTA polymer chain is found. Furthermore, weak PPTA-related fragments  $[\text{C}_6\text{H}_n]^-$  ( $n = 0-4$ ),  $[\text{C}_6\text{H}_n-\text{C}]^-$  ( $n = 0-2$ ),  $[\text{C}-\text{C}_6\text{H}_n-\text{C}]^-$  ( $n = 0-2$ ),  $[\text{C}_6\text{H}_4-\text{CON}]^-$ ,  $[\text{C}_6\text{H}_4\text{NH}_2]^-$ , and  $[\text{CO}-\text{C}_6-\text{CON}]^-$  due to aromatic ions are observed in the higher mass range. Significant “fingerprint” organic fragment ions are capable of providing structural information about the repeating unit of PPTA [i.e.,  $(-\text{CO}-\text{C}_6\text{H}_4-\text{CO}-\text{NH}-\text{C}_6\text{H}_4-\text{NH}-)_n$ ].

After treatment with 30 W  $\text{NH}_3$ -plasma for 3 min, the negative ion spectrum is similar to that of the control fiber. But new peaks can be observed in the

mass of 108 and 112 amu [Fig. 3(b)]. These peaks can be assigned to  $[\text{C}_6\text{H}_4(\text{NH}_2)_2]^-$  and  $[\text{C}-\text{C}_6(\text{NH}_2)-\text{C}]^-$ . This may indicate that at least primary amino groups are formed after  $\text{NH}_3$ -plasma treatment. Figure 3(c) shows the negative ion spectrum of Kevlar 49 fiber treated by 30 W  $\text{O}_2$ -plasma for 3 min. In comparison with Figure 3(a), many peaks disappeared in the mass ranges of 76, 84–86, 92, and 96–98 amu. There is a lack of aromatic ring fragments and this means that the high concentration of oxygen in plasma led to extensive damage of the aromatic ring and polymer backbone.<sup>26</sup> After treatment with  $\text{H}_2\text{O}$ -plasma at 30 W for 3 min [Fig. 3(d)], relatively high intensities of peaks at  $\text{O}^-$  (16),  $\text{OH}^-$  (17), and  $\text{O}_2^-$  (32) are found, and there are many new peaks in the mass of 107  $[\text{C}_6\text{H}(\text{OH})_2]^-$ , 109  $[\text{C}_6\text{H}_3(\text{OH})_2]^-$ , 110  $[\text{C}_6\text{H}_4(\text{OH})_2]^-$ , 114  $[\text{C}-\text{C}_6\text{H}(\text{OH})-\text{C}]^-$ , 119  $[\text{C}-\text{C}_6\text{H}(\text{OH})_2]^-$ , and 136  $[\text{C}-\text{C}_6\text{H}(\text{OH})_3]^-$ . These oxygen-containing fragments result from the large amount of oxygen atom incorporated into the fiber surface.<sup>25</sup>

### Chemical Treatment

After treatment with 0.25% chlorosulfonic acid for 2.5 min, the spectra (not shown) reveal the peak of  $\text{C}_6\text{H}_3\text{S}^-$  (107). This means that the sulfur-containing functionality was introduced into the fiber surface by chlorosulfonation treatment.

### Interlaminar Fracture Energy

The  $G_{\text{IC}}$  values for the untreated and treated aramid/epoxy composites, determined from eq. (1), is a function of the crack length. All  $G_{\text{IC}}$  vs. crack length graphs exhibited the characteristic  $R$  curves associated with fiber bridging. The results show that

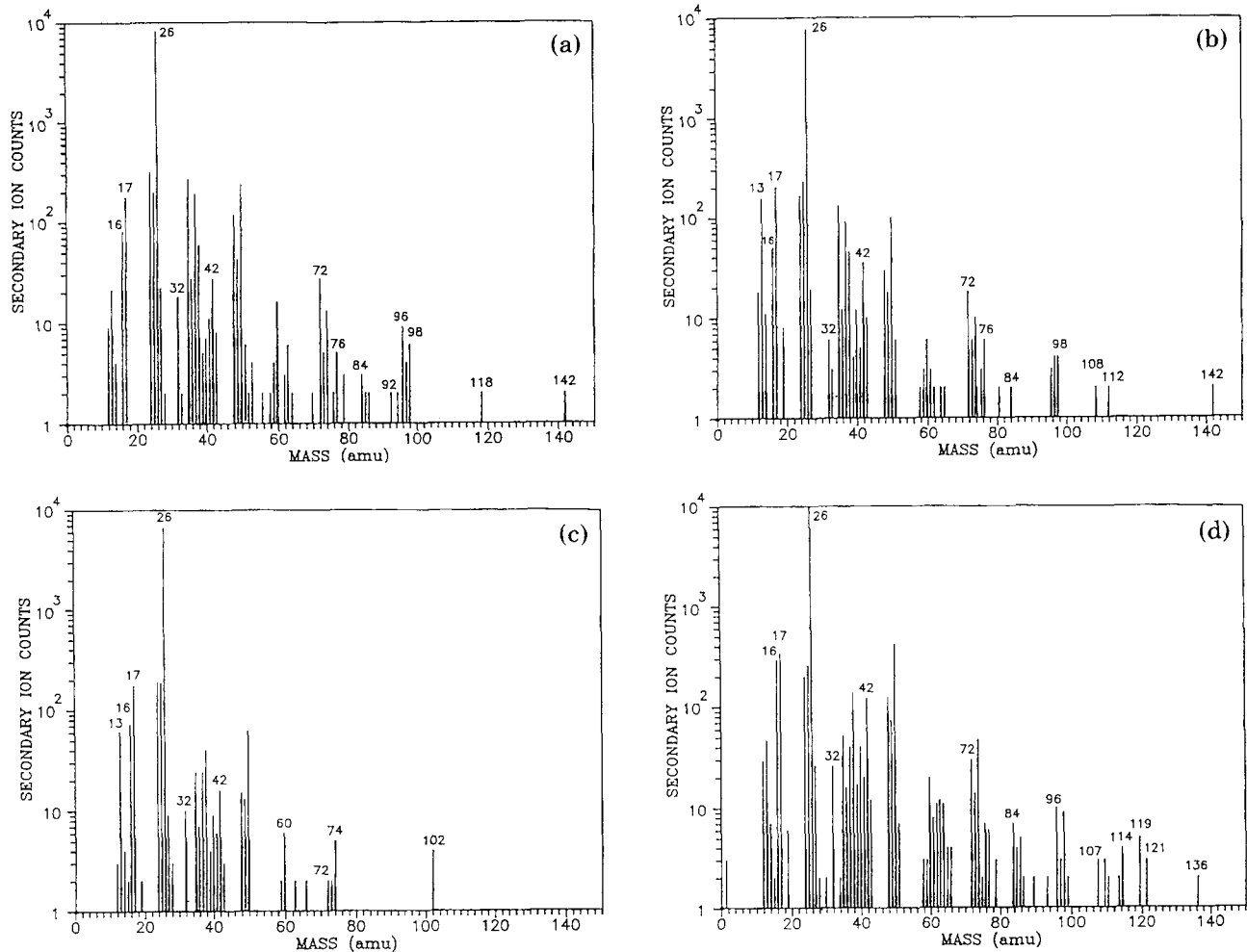


**Figure 3** (a) Negative SSIMS spectrum of untreated (control) Kevlar 49 fibers. (b) Negative SSIMS spectrum of Kevlar 49 fibers treated by  $\text{NH}_3$ -plasma at 30 W for 3 min. (c) Negative SSIMS spectrum of Kevlar 49 fibers treated by  $\text{O}_2$ -plasma at 30 W for 3 min. (d) Negative SSIMS spectrum of Kevlar 49 fibers treated by  $\text{H}_2\text{O}$ -plasma at 30 W for 3 min.

there is no significant change in interlaminar fracture energy after plasma and chemical treatments (Figs. 4 and 5). It was found that the interlaminar fracture energy of the composite is sensitive to and controlled by the fracture toughness of the matrix resin up to a limiting resin toughness, beyond which the interlaminar fracture energy does not increase in the same proportion as that of the matrix.<sup>4</sup> So, the fiber/matrix interfacial bond strength is only a minor factor to  $G_{\text{IC}}$  values for fiber composites. The appearance of large internal cracks in some filaments could only happen at a higher concentration of chlorosulfonic acid. This may cause lower  $G_{\text{IC}}$  values because the crack growth occurred on the filaments, rather on the matrix or interface. Otherwise, there is no significant change in  $G_{\text{IC}}$  values.

## Interlaminar Shear Strength

### Plasma Treatment

The interlaminar shear strength (ILSS) of the aramid/epoxy composites was calculated from eq. (2). Results of the test are shown in Tables III and IV. A marked increase in the apparent ILSS obtained for the laminate prepared from plasma-treated fiber is due to an increase in the fiber/matrix interface strength. The effects of the treatment time on the ILSS of the fiber treated by various plasma at a power level of 30 W is shown in Figure 6. However, a treatment time longer than 5 min did not increase the ILSS further in the case of the plasma treatment. The degree of the increase in ILSS among different plasmas is  $\text{NH}_3 > \text{O}_2 > \text{H}_2\text{O}$ . The increase in the

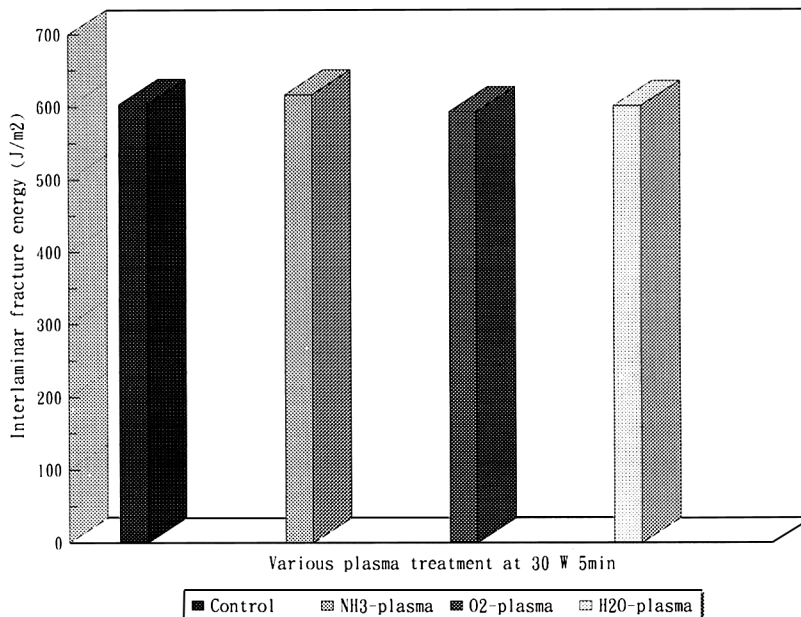


**Figure 4** Dependence of the critical strain energy release rate of the Kevlar 49 fiber-epoxy system on the various plasma at 30 W power for 5 min.

ILSS of the plasma-treated samples can be elucidated in that the plasma treatments incorporated some newly formed functionalities onto the fiber surface which would improve the wettability and increase the surface energy of the fiber surface. Other possible factors such as chemical bonding between the newly formed functionalities and epoxy resin may also be contributing to the increase in ILSS.

**Chemical Treatment**

Figure 7 shows the effect of the chlorosulfonic acid concentration and treatment time on the ILSS. The ILSS was markedly improved by 0.1 and 0.25% chlorosulfonic acid treatment for 30 s. But higher concentrations of chlorosulfonic acid and longer reaction times caused a lower ILSS. This may be due

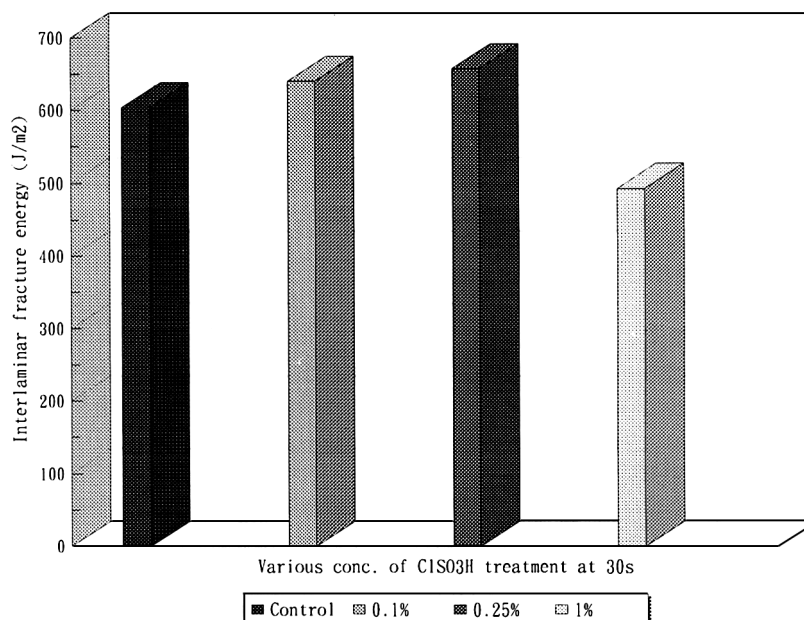


**Figure 5** Dependence of the critical strain energy release rate of the Kevlar 49 fiber-epoxy system on the various concn of ClSO<sub>3</sub>H at 30 s.



**Table III Mechanical Properties of Aramid/Epoxy Composites After Plasma Treatment**

Plasma Treatment	Interlaminar Fracture Energy ( $\text{J m}^{-2}$ )	Interlaminar Shear Strength (MPa)	T-peel Strength (gw/cm)
None	$604 \pm 67$	$20.6 \pm 1.2$	$350 \pm 25$
NH <sub>3</sub> -plasma			
15 s at 30 W	—	$25.3 \pm 0.2$	$550 \pm 15$
1 min at 30 W	—	$30.9 \pm 0.5$	$570 \pm 30$
5 min at 30 W	$617 \pm 52$	$33.1 \pm 1.2$	$617 \pm 32$
10 min at 30 W	—	$30.6 \pm 0.9$	$583 \pm 26$
O <sub>2</sub> -plasma			
15 s at 30 W	—	$25.6 \pm 1.5$	$400 \pm 15$
1 min at 30 W	—	$27.4 \pm 0.6$	$533 \pm 26$
5 min at 30 W	$594 \pm 85$	$29.2 \pm 1.3$	$566 \pm 30$
10 min at 30 W	—	$28.9 \pm 1.1$	$573 \pm 28$
H <sub>2</sub> O-plasma			
15 s at 30 W	—	$22.8 \pm 1.1$	$450 \pm 27$
1 min at 30 W	—	$25.0 \pm 0.3$	$466 \pm 25$
5 min at 30 W	$602 \pm 62$	$27.5 \pm 0.6$	$533 \pm 21$
10 min at 30 W	—	$22.5 \pm 0.3$	$433 \pm 24$

to that the chlorosulfonic acid is capable of penetrating the fiber and causing significant disruption of the microstructure and strength of the fiber. In

addition to the interfacial bonding, the fiber strength is also an important factor for the ILSS in the short-beam method.

**Table IV Mechanical Properties of Aramid/Epoxy Composites After Chemical Treatment**

Plasma Treatment	Time (min)	Interlaminar Fracture Energy ( $\text{J m}^{-2}$ )	Interlaminar Shear Strength (MPa)	T-peel Strength (gw/cm)
None		$604 \pm 67$	$20.6 \pm 1.2$	$350 \pm 25$
Chlorosulfonation concn (wt %)				
0.1	0.25	—	$27.2 \pm 0.6$	$413 \pm 23$
0.1	0.5	$640 \pm 72$	$31.6 \pm 0.3$	$533 \pm 21$
0.1	2.5	—	$27.3 \pm 0.2$	$520 \pm 27$
0.1	5	—	$25.1 \pm 0.4$	$346 \pm 21$
0.25	0.25	—	$25.1 \pm 0.3$	$467 \pm 17$
0.25	0.5	$657 \pm 63$	$31.4 \pm 0.5$	$480 \pm 21$
0.25	2.5	—	$19.4 \pm 0.7$	$427 \pm 23$
0.25	5	—	$15.4 \pm 0.3$	$213 \pm 16$
1	0.25	—	$20.0 \pm 0.3$	$293 \pm 17$
1	0.5	$492 \pm 67$	$15.0 \pm 0.7$	$237 \pm 13$
1	2.5	—	$10.0 \pm 0.7$	$200 \pm 10$
1	5	—	$8.0 \pm 0.6$	$146 \pm 10$
Chlorosulfonation (concn 0.25% for 15 s)/ glycine (concn 1% for 15 min)		—	$26.3 \pm 0.4$	$492 \pm 17$
Chlorosulfonation (concn 0.25% for 15 s)/ deionized water (15 min)		—	$25.71 \pm 0.5$	$485 \pm 21$
Chlorosulfonation (concn 0.25% for 15 s)/ ethylenediamine (concn 15% for 15 min)		—	$27.68 \pm 0.5$	$505 \pm 21$
Chlorosulfonation (concn 0.25% for 15 s)/ 1-butanol (concn 15% for 15 min)		—	$24.92 \pm 0.4$	$445 \pm 17$

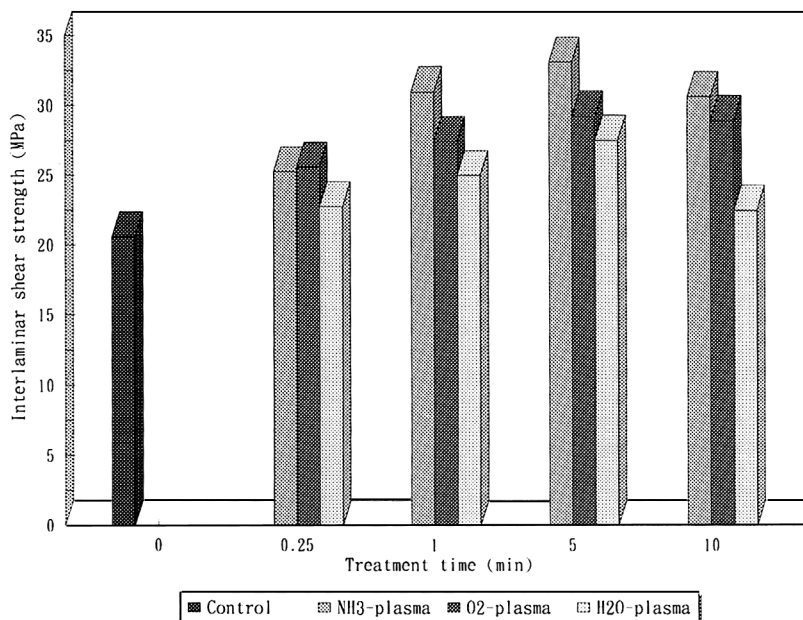


**Figure 6** Dependence of the interlaminar shear strength of the Kevlar 49 fiber-epoxy system on the treatment time of fiber treated by various plasma at 30 W power level.

In this study, 0.25% chlorosulfonic acid and 15 s treatment time were selected as the initial conditions prior to further reaction treatment. Table IV shows the ILSS of the composite which was posttreated with glycine, deionized water, ethylenediamine, and 1-butanol. The results suggest that the posttreatment does not introduce reactive groups into the fiber surface effectively and may cause the fiber strength decrease. The surface modification with reactive functional groups and improved the bonding of aramid fibers in epoxy composites can be attained by chlorosulfonation that does not require subsequent reaction with any reagents.

## T-peel Strength

### Plasma Treatment

Composite laminates for preliminary evaluation of the T-peel strength were performed by ASTM-D-1876-72. Figure 8 shows the T-peel strength for composites containing untreated and plasma-treated fibers. There is no significant difference in the tensile strength between the control and plasma-treated Kevlar 49 fiber.<sup>11</sup> Hence, the increase in T-peel strength of the two-ply structure is considered to be due to significantly enhanced bonding at the interface. These results indicate that at least some covalent bonds between the new functional groups at the plasma-treated fiber surface and the epoxy resin were formed. The degree of the increase in T-peel

strength among different plasmas is  $\text{NH}_3 > \text{O}_2 > \text{H}_2\text{O}$ . The T-peel strength was shown to increase with increasing treatment time up to 5 min, after which there was no further increase. These results are similar to interlaminar shear strength after plasma treatment.

### Chemical Treatment

The effect of the chemical treatment on the T-peel strength is shown in Figure 9. These results suggest that an improvement is realized by the introduction of  $-\text{SOCl}_2$  groups, but higher concentrations of chlorosulfonic acid and longer reaction times would not enhance the T-peel strength further. This may be due to that the fiber strength decreases [Fig. 2(c) and (d)] with unsuitable treatment. The effects of the chemical treatment of the fiber surfaces on the T-peel strength are also quite similar to that of the interlaminar shear strength.

## Fracture Surface Analysis of the T-peel Test Specimens

### Plasma Treatment

The fracture surfaces of the T-peel test specimens were examined by SEM. As shown in Figure 10(a), the untreated fiber surface after the T-peel test is quite smooth. No resin remains on the surface and only a few torn filament skins appeared. Therefore,

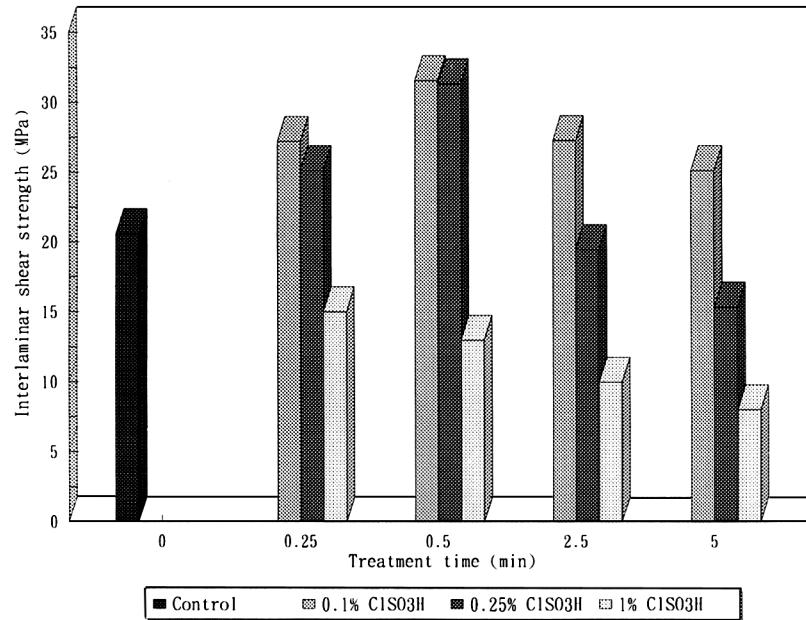


**Figure 7** Dependence of the interlaminar shear strength of the Kevlar 49 fiber-epoxy system on the treatment time of fiber treated by various concn of CISO<sub>3</sub>H.

the fracture mode of the untreated composite is at the interface of the fiber/matrix. This means that the interfacial bonding is poor and the interface structure cannot transfer stress effectively.

The fracture surfaces of the plasma-treated specimens are shown in Figure 10(b)-(d). There

are significant differences between the failure surface of untreated peel specimens and those of specimens prepared from plasma-treated fiber. After 30 W NH<sub>3</sub>-plasma treatment for 10 min [Fig. 10(b)], the fracture surface shows some fiber skins and fracture resin left in the resin grooves, which

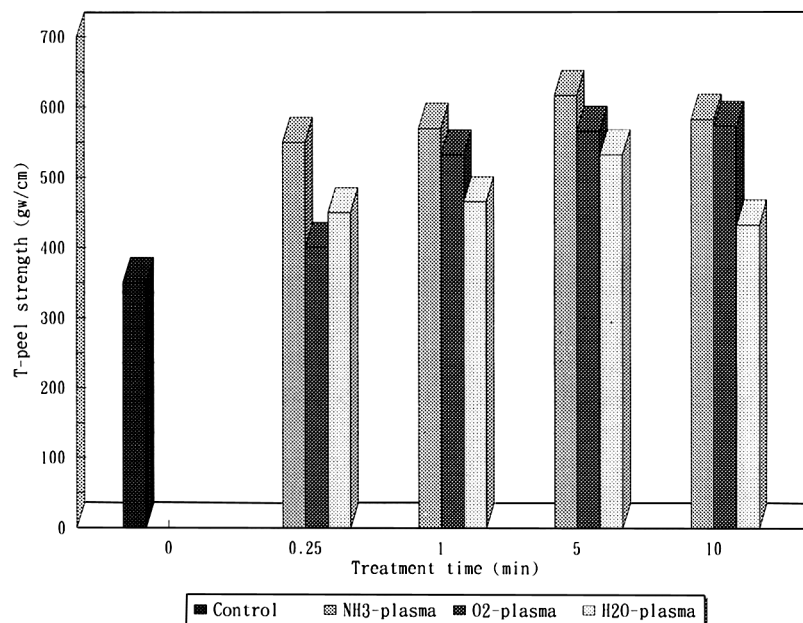


**Figure 8** Dependence of T-peel strength of the Kevlar 49 fiber-epoxy system on the treatment time of fiber treated by various plasma at 30 W power level.

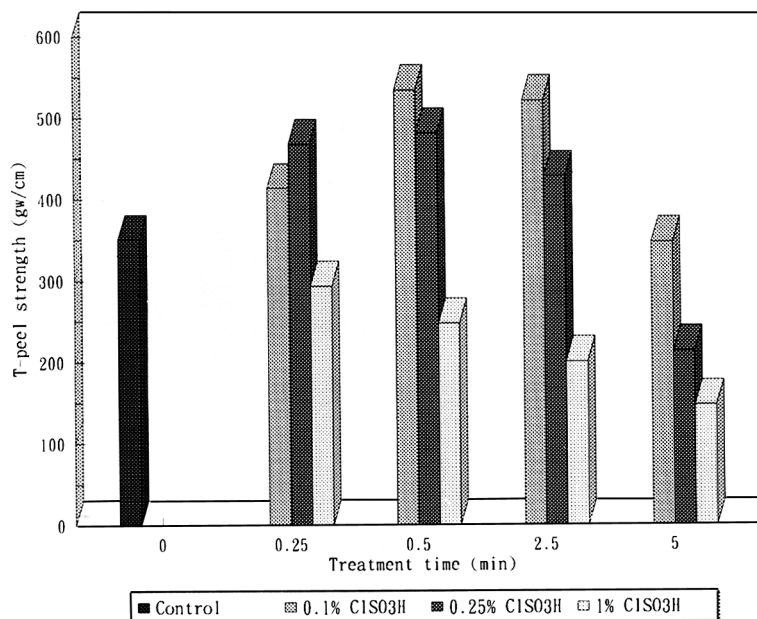


**Figure 9** Dependence of T-peel strength of the Kevlar 49 fiber-epoxy system on the treatment time of fiber treated by various concn of ClSO<sub>3</sub>H.

are not regular and smooth. After 30 W O<sub>2</sub>-plasma treatment for 10 min [Fig. 10(c)], the fracture surface reveals axially split filaments and torn filament skins. A fibril-like structure of the fracture surface is also observed in the case of the H<sub>2</sub>O-plasma treatment [Fig. 10(d)]. At the same control condition, the fracture surface of the H<sub>2</sub>O-plasma treatment is more regular and smoother than that of the NH<sub>3</sub>- and O<sub>2</sub>-plasma treatment. However, the peeling of fibrils in the T-peel test specimen shows that the interfacial bond strength is greater than is the filament internal strength. This may be due to the improvement of the interfacial bonding and the weakening of the skin-core strength by the plasma treatment.

### Chemical Treatment

The surface of the chemical-treated specimen after the T-peel test was quite similar to the fracture surface of the plasma-treated specimen. But using higher concentrations of chlorosulfonic acid and longer reaction times, large internal cracks [Fig. 11(a) and (b)] appeared in some filaments and torn filament skins over extensive distances were also observed. This means that the failure mode changed to the fiber fibrillation and the chlorosulfonic acid may penetrate inside the fiber, destroying the structure of the fiber. So, the choice of the conditions in chemical treatment is very important.

### CONCLUSIONS

Plasma and chemical treatment of aramid fibers results in changes in the interface sensitive mechanical properties of aramid epoxy composites. Interlaminar shear strength and T-peel strength between the fiber and epoxy resin were markedly improved by plasma treatment and chlorosulfonation. It was suggested that covalent bonding of the epoxy resin with functional groups on fiber surfaces could be a major factor in the interfacial bond strength of the composites. But the decrease in ILSS and T-peel strength was significant when the fiber was treated at a higher concentrations of chlorosulfonic acid or longer reaction times. Such treatment caused the fiber surfaces to be etched vigorously and the decrease in fiber strength. The postchemical treatments did not further change the ILSS and T-peel strength. This may be due to that the posttreatment did not introduce reactive groups into the fiber surface effectively and caused the fiber strength decrease. Because the fiber/matrix interfacial bond strength is only a minor contributor to  $G_{IC}$  and the  $G_{IC}$  values of the composite depends mainly on the fracture toughness of the matrix resin, any pretreatment of the reinforced fiber would not significantly change the  $G_{IC}$  values. SEM observations show that the improvement of fiber/matrix interfacial bond strength is often accompanied by a change in the fracture mode from

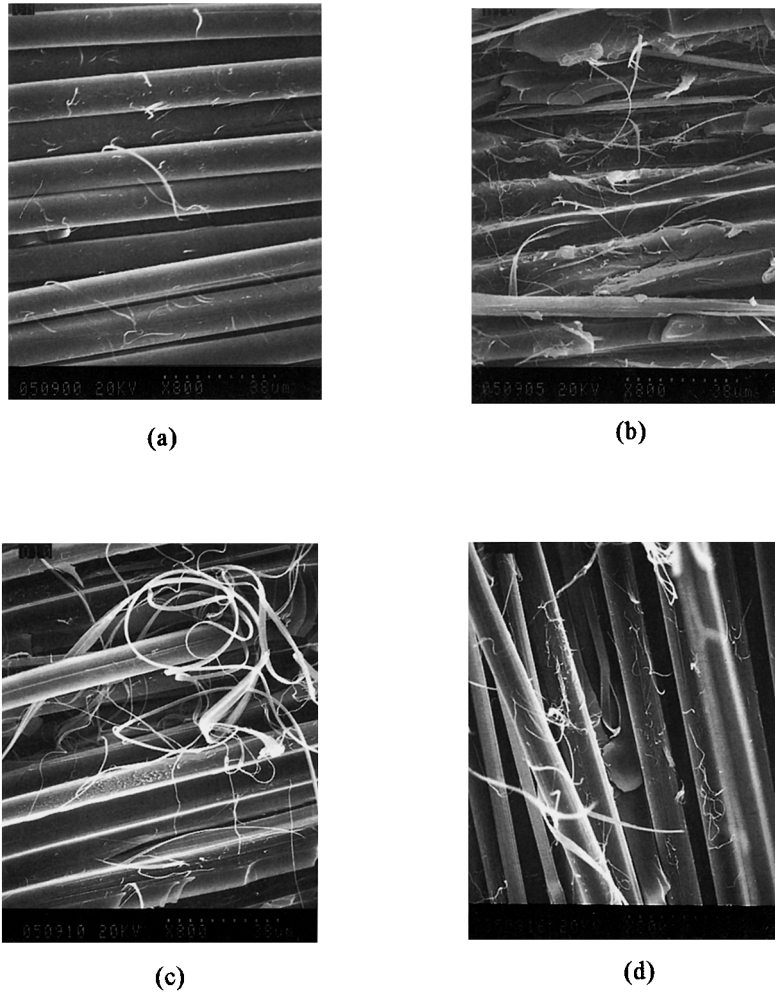


**Figure 10** Fracture surfaces of T-peel test specimens for Kevlar 49 fiber-epoxy system: (a) control; (b) treated by NH<sub>3</sub>-plasma at 30 W for 10 min; (c) treated by O<sub>2</sub>-plasma at 30 W for 10 min; (d) treated by H<sub>2</sub>O-plasma at 30 W for 10 min.

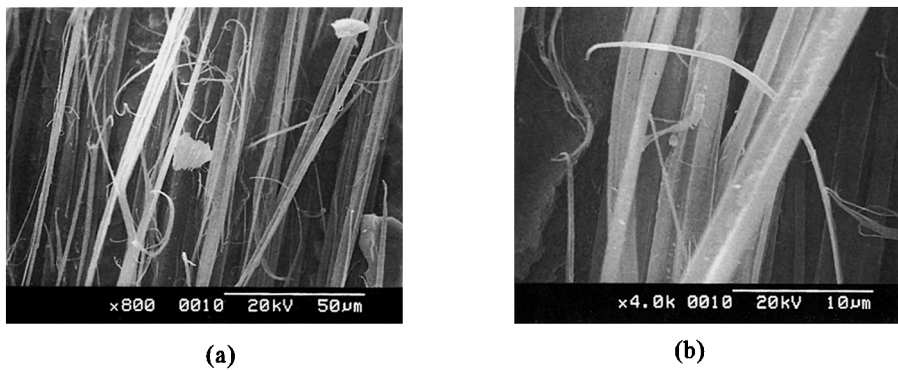


**Figure 11** Fracture surfaces of T-peel test specimens for Kevlar 49 fiber-epoxy system treated by 1% ClSO<sub>3</sub>H for (a) 2.5 min and (b) 5 min.

the failure at the interface of fiber/epoxy resins to the fiber fibrillation and the resins.

## REFERENCES

1. M. R. Wertheimer and H. P. Schreiber, *J. Appl. Polym. Sci.*, **26**, 2087 (1981).
2. L. S. Penn and T. K. Liao, *Compos. Technol. Rev.*, **6**, 133 (1984).
3. K. Küpper and P. Schwartz, *J. Adhes. Sci. Technol.*, **5**, 165 (1991).
4. J. R. Brown, P. J. C. Chappell, and Z. Mathys, *J. Mater. Sci.*, **26**, 4172 (1991).
5. Q. Wang, S. Kaliaguine, and A. Ati-Kadi, *J. Appl. Polym. Sci.*, **48**, 121 (1993).
6. L. Y. Yuan, S. S. Shyu, and J. Y. Lai, *J. Appl. Polym. Sci.*, **42**, 2525 (1991).
7. L. Y. Yuan, S. S. Shyu, and J. Y. Lai, *Compos. Sci. Technol.*, **45**, 9 (1992).
8. G. S. Sheu, T. K. Lin, S. S. Shyu, and J. Y. Lai, *J. Adhes. Sci. Technol.*, **8**, 511 (1994).
9. G. S. Sheu and S. S. Shyu, *J. Adhes. Sci. Technol.*, **8**, 531 (1994).
10. G. S. Sheu and S. S. Shyu, *J. Adhes. Sci. Technol.*, **8**, 1027 (1994).
11. G. S. Sheu and S. S. Shyu, *Compos. Sci. Technol.*, **52**, 489 (1994).
12. Y. Wu and G. C. Tesoro, *J. Appl. Polym. Sci.*, **31**, 1041 (1986).
13. L. S. Penn and B. Jutis, *J. Adhes.*, **30**, 67 (1987).
14. M. Takayanagi, S. Ueta, W.-Y. Lei, and K. Koga, *Polym. J.*, **19**, 467 (1987).
15. L. S. Penn, G. C. Tesoro, and H. X. Zhou, *Polym. Compos.*, **9**, 184 (1988).
16. M.-L. Chen, S. Ueta, and M. Takayanagi, *Polym. J.*, **20**, 673 (1988).
17. C. T. Chou and L. S. Penn, *J. Adhes.*, **36**, 125 (1991).
18. R. Benrashid and G. C. Tesoro, *Text. Res. J.*, **60**, 334 (1990).
19. F. P. M. Mercx and P. J. Lemstra, *Polym. Commun.*, **31**, 252 (1990).
20. V. Ravichandran and S. K. Obendorf, *J. Adhes. Sci. Technol.*, **6**, 1303 (1992).
21. D. J. Vaughan, *Polym. Eng. Sci.*, **18**, 167 (1978).
22. A. G. Andreopoulos, *J. Appl. Polym. Sci.*, **38**, 1053 (1989).
23. R. E. Allred, E. W. Merrill, and D. K. Roylane, in *Molecular Characterization of Composite Interfaces*, H. Ishida and G. Kumar, Eds., Plenum Press, New York, 1985, pp. 333-375.
24. L. Penn and F. Larsen, *J. Appl. Polym. Sci.*, **23**, 59 (1979).
25. L. M. Ferreiro, D. W. Ernie, and J. F. Evans, *J. Van. Sci. Technol.*, **A5**, 2280 (1987).
26. E. Occhiello, F. Garbassi, and M. Morra, *Surf. Sci.*, **211/212**, 218 (1989).

Received October 7, 1995

Accepted June 1, 1996